

Kantorovich vs. Monge: A Numerical Classification of Extremal Multi-Marginal Mass Transports on Finite State Spaces

Daniela Vögler*

Abstract. We analyze the validity of Monge’s ansatz regarding the symmetric multi-marginal Kantorovich optimal transport problem on finite state spaces, with uniform-marginal constraint.

The class of Monge states reduces the number of unknowns from combinatorial in both N and ℓ to linear in N and ℓ , where N is the number of marginals and ℓ the number of states. Unfortunately, this low-dimensional ansatz space is insufficient, i.e., there exist cost functions such that the corresponding multi-marginal optimal transport problem does not admit a Monge-type optimizer. We will analyze this insufficiency numerically by utilizing the convex geometry of the set of admissible trial states for symmetric respectively pairwise-symmetric cost functions.

We further consider a model problem of optimally coupling N marginals on three states with respect to a pairwise-symmetric cost function. The restriction to a state space of three elements allows us to visually compare Kantorovich’s to Monge’s ansatz space. This visual comparison includes a consideration of the volumetric ratio.

Keywords: optimal transport, Monge’s ansatz, N-representability, Birkhoff-von Neumann theorem, density functional theory

Mathematics Subject Classification: 49J40, 49K30, 52B12, 49S05

Acknowledgments: The author thanks Gero Friesecke and Sören Behr for helpful discussions.

1 Introduction

In general multi-marginal Kantorovich optimal transport problems aim at coupling N probability measures $\lambda^{(1)}, \dots, \lambda^{(N)}$ optimally with respect to a given cost function c (see (1.1) for a discrete symmetric optimal transport problem). These problems arise in various fields of research, ranging from economics [8, 11] through mathematical finance [2, 19] and image processing [1, 32] to electronic structure [13, 6].

One of the central questions in the theory of optimal transportation is: Under which assumptions exists an optimal coupling that is supported on a graph (over the first variable)? Such optimizers are then called Monge-solutions (see (1.5) - (1.7)). In the case of two marginals this question is well understood; the existence of Monge-solutions is always respectively under very general conditions guaranteed (see the renowned Birkhoff-von Neumann theorem [4, 36] regarding finite state spaces respectively, e.g., [35] regarding continuous state spaces). For multiple marginals the understanding of this question does not reach the same generality. However, there are isolated examples for Monge- and non-Monge-solutions. For the former, see [22, 7, 28, 13, 6, 12] as well as the fundamental paper by Gangbo and Świąch [20] for an interesting selection. For the latter, we refer the interested reader to

*Faculty of Mathematics, Technische Universität München, voegler@ma.tum.de, +49-89-289-17900 (Tel.), +49-89-289-17932 (Fax)

[9, 29, 17, 30, 14, 27, 21, 16] regarding continuous state spaces as well as to [15, 25, 26, 16] regarding finite state spaces.

The goal of this paper is to investigate the validity of Monge's ansatz regarding the symmetric multi-marginal Kantorovich optimal transport problem on finite state spaces

$$\begin{aligned} \text{Minimize } & \int_{X^N} c(x_1, \dots, x_N) d\gamma(x_1, \dots, x_N) \\ & \text{over } \gamma \in \mathcal{P}_{\text{sym}}(X^N) \text{ subject to } \gamma \mapsto \bar{\lambda}. \end{aligned} \quad (1.1)$$

Here X denotes a finite state space as defined in (1.2), $c : X^N \rightarrow \mathbb{R} \cup \{+\infty\}$ an arbitrary symmetric cost function, $\bar{\lambda}$ the uniform marginal as defined in (1.3) and $\mathcal{P}_{\text{sym}}(X^N)$ the set of symmetric probability measures on X^N , where a probability measure γ on X^N is symmetric if

$$\begin{aligned} \gamma(A_1 \times \dots \times A_N) &= \gamma(A_{\sigma(1)} \times \dots \times A_{\sigma(N)}) \\ & \text{for all subsets } A_1, \dots, A_N \text{ of } X \text{ and all permutations } \sigma. \end{aligned}$$

Any $\gamma \in \mathcal{P}_{\text{sym}}(X^N)$ fulfills $\gamma \mapsto \bar{\lambda}$ if and only if γ has equal one-point marginals $\bar{\lambda}$, i.e.,

$$\gamma(X^{k-1} \times A_k \times X^{N-k}) = \bar{\lambda}(A_k) \text{ for all subsets } A_k \text{ of } X \text{ and all } k \in \{1, \dots, N\}.$$

Multi-marginal optimal transport problems of form (1.1) were already considered in [18] and [16]. While [16] discusses the validity of Monge's approach in the setting of 3 marginals and 3 sites, [18] introduces a sufficient ansatz space for problem (1.1) (see Section 2 as well as Remark 3.5 for information about the content of these papers). The present paper accompanies these previous considerations. In particular, some of the used nomenclature and notation is already introduced there.

For finite state spaces

$$X = \{a_1, \dots, a_\ell\} \quad (1.2)$$

consisting of ℓ distinct points a_1, \dots, a_ℓ , the uniform probability measure

$$\bar{\lambda} = \sum_{i=1}^{\ell} \frac{1}{\ell} \delta_{a_i} \quad (1.3)$$

on X is the prototypical marginal. The corresponding multi-marginal Kantorovich optimal transport problems, i.e., problems of form (1.1) with $\mathcal{P}(X^N)$ replacing $\mathcal{P}_{\text{sym}}(X^N)$, appear directly as assignment problems (see [34, 5] for reviews) and arise from continuous problems via equi-mass discretization [10]. Then, an optimal coupling $\gamma \in \mathcal{P}(X^N)$ of the N marginals $\bar{\lambda}, \dots, \bar{\lambda}$ is a Monge-solution if

$$\gamma = \sum_{\nu=1}^{\ell} \frac{1}{\ell} \delta_{T_1(a_\nu)} \otimes \dots \otimes \delta_{T_N(a_\nu)} \text{ for } N \text{ permutations } T_1, \dots, T_N : X \rightarrow X, \quad (1.4)$$

where $T : X \rightarrow X$ is a permutation if there exists a permutation of indices $\tau : \{1, \dots, \ell\} \rightarrow \{1, \dots, \ell\}$ such that $T(a_\nu) = a_{\tau(\nu)}$ for all $\nu \in \{1, \dots, \ell\}$. Demanding that the T_k s are permutations ensures that γ is indeed a coupling of $\bar{\lambda}, \dots, \bar{\lambda}$: $T : X \rightarrow X$ is a permutation

if and only if it pushes the uniform measure forward to itself, i.e., $T_{\#}\bar{\lambda} = \bar{\lambda}$. Here for any probability measure $\lambda = \sum_{\nu=1}^{\ell} \lambda_{\nu} \delta_{a_{\nu}}$ on X and any map $T : X \rightarrow X$ the push-forward $T_{\#}\lambda$ of λ under T is defined by $T_{\#}\lambda = \sum_{\nu=1}^{\ell} \lambda_{\nu} \delta_{T(a_{\nu})}$. One may choose $T_1 = \text{id}$, i.e., $T_1(a) = a$ for all $a \in X$, by re-ordering the sum in (1.4).

Regarding (1.1) an admissible trial state $\hat{\gamma}$ is referred to as a (symmetrized) Monge state if it is the symmetrization of a probability measure γ of form (1.4), i.e.,

$$\hat{\gamma} = \sum_{\nu=1}^{\ell} \frac{1}{\ell} S \delta_{T_1(a_{\nu})} \otimes \cdots \otimes \delta_{T_N(a_{\nu})} \quad (1.5)$$

such that

$$T_k \# \bar{\lambda} = \bar{\lambda} \text{ for all } k \in \{1, \dots, N\}, \quad (1.6)$$

or equivalently,

$$T_1, \dots, T_N : X \rightarrow X \text{ are permutations.} \quad (1.7)$$

Here S denotes the linear symmetrization operator in N variables as defined in (2.4). Probability measures on X^N of form (1.5)-(1.7) are also said to be of Monge-type or in Monge-form and restricting the minimization problem (1.1) to such measures yields the corresponding Monge problem.

A guarantee for the existence of a Monge-solution would allow us to utilize the Monge approach (1.5)-(1.7) in order to reduce the number of unknowns in (1.1) from combinatorial in both N and ℓ to linear in N and ℓ . Unfortunately, for multiple marginals the Monge ansatz is, again, not sufficient: In [16] an example for a symmetric cost function $c : X^3 \rightarrow \mathbb{R} \cup \{+\infty\}$ such that there exists a unique minimizer of problem (1.1) that is not of Monge-type is given. In Section 2, we will quantify this insufficiency of Monge's approach by utilizing the convex geometry of the set of admissible trial states.

Note that the restriction to symmetric probability measures in problem (1.1) is motivated by a physical application. Modeling the electronic structure of a molecule with N electrons in a discretized setting, is a prototypical application of multi-marginal optimal transport on finite state spaces. In this context, X corresponds to a set of ℓ discretization points in \mathbb{R}^3 and any coupling γ of the N marginals $\bar{\lambda}, \dots, \bar{\lambda}$ describes a joint probability distribution regarding the electron positions in an N -electron molecule. Then the marginal condition ensures that each discretization point is occupied equally often and the cost function $c : X^N \rightarrow \mathbb{R} \cup \{+\infty\}$ embodies the electron interaction energy. As electrons are indistinguishable the considered cost functions are usually symmetric, i.e., invariant under argument permutation. These symmetric cost functions are 'dual' to the set of symmetric probability measures on the product space X^N in the following sense: There always exists an optimal coupling of $\bar{\lambda}, \dots, \bar{\lambda}$ that is symmetric.

The interaction energy between electrons often displays pairwise structure, i.e., $c(x_1, \dots, x_N) = \sum_{1 \leq i < j \leq N} v(x_i, x_j)$, with the Coulomb cost $\sum_{1 \leq i < j \leq N} \frac{1}{|x_i - x_j|}$ being the prototypical example. Here $|\cdot|$ is the Euclidean norm in \mathbb{R}^d . As discussed in Section 3, this pairwise structure allows us to reformulate the multi-marginal optimal transport problem (1.1) as

$$\text{Minimize } \int_{X^2} v(x, y) d\mu(x, y) \text{ over } \mu \in \mathcal{P}_{N\text{-rep}}(X^2) \text{ subject to } \mu \mapsto \bar{\lambda}. \quad (1.8)$$

This reformulated problem was initially introduced in [17]. In (1.8), $\mathcal{P}_{N\text{-rep}}(X^2) \subseteq \mathcal{P}(X^2)$ can be interpreted as a 'reduced version' of $\mathcal{P}_{\text{sym}}(X^N)$.

The above mentioned cost function $c : X^3 \rightarrow \mathbb{R} \cup \{+\infty\}$ in [16], which establishes the insufficiency of Monge's ansatz regarding problem (1.1), is of pairwise structure. It immediately follows that there is no 'reduced Monge state' that solves problem (1.8). In this sense the Monge ansatz is also insufficient for the reformulated problem (1.8). In Section 3, we will make use of the convex geometry of the new set of admissible trial states in order to quantify this insufficiency of Monge's ansatz.

Finally, in Section 4, we will consider a model problem of optimally coupling the N marginals $\bar{\lambda}, \dots, \bar{\lambda}$ with respect to a cost function of pairwise symmetric structure, where the finite state space X consists only of three states, i.e., $X = \{a_1, a_2, a_3\}$. In particular $\bar{\lambda}$ is the uniform probability measure on $\{a_1, a_2, a_3\}$ and the domain of the cost function is given by $\{a_1, a_2, a_3\}^N$. The present setting allows us to draw a visual comparison between Kantorovich's and Monge's ansatz as depicted in Figure 1. We further compare both optimal transport approaches by volume of (the convex hull of) the respective set of admissible trial states and establish a computationally simple upper bound on the optimal value in (1.8).

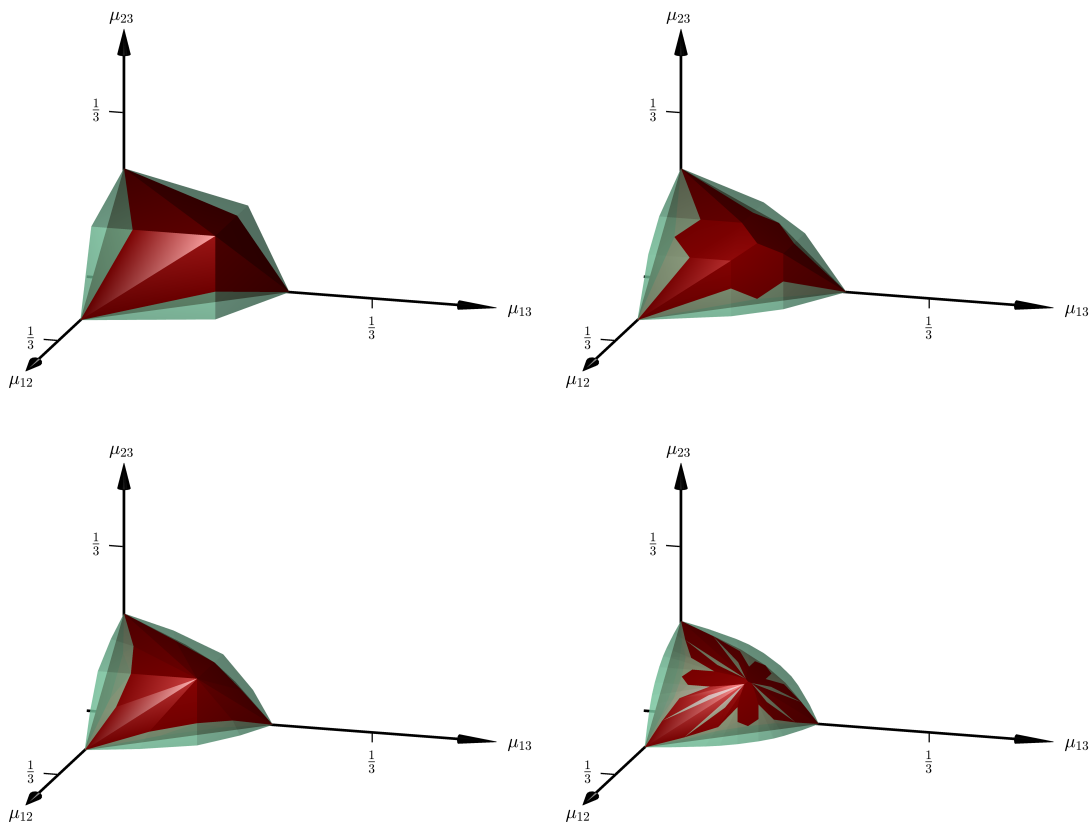


Figure 1: The reduced Kantorovich (see (3.4)) respectively Monge (see (3.8)) polytope for N marginals and 3 states is visualized for $N = 3$ (top-left), 4 (top-right), 6 (bottom-left) and 10 (bottom-right) in green respectively red. The elements $(\mu_{ij})_{i,j=1}^3$ of the polytopes are parametrized by their off-diagonal entries μ_{12}, μ_{13} and μ_{23} . If a two-dimensional face of the reduced Monge polytope belongs to the boundary of the reduced Kantorovich polytope the occupied area is depicted in red.

2 Classification of the Extreme Points of a Kantorovich Polytope

Throughout the paper we will consider the finite state space X given by (1.2). We will denote the set of probability measures on X as $\mathcal{P}(X)$. Each such probability measure $\lambda \in \mathcal{P}(X)$ can be canonically identified with a vector in \mathbb{R}^ℓ in the following manner

$$\lambda_i := \lambda(a_i).$$

The vector $(\lambda_1, \dots, \lambda_\ell)$ fulfills $\sum_{i=1}^\ell \lambda_i = 1$ and $\lambda_i \geq 0$ for $i \in \{1, \dots, \ell\}$ and is therefore an element of the unit simplex. The probability measure λ can then be written in the following manner

$$\lambda = \sum_{i=1}^{\ell} \lambda_i \delta_i,$$

where here and below we use the shorthand notations

$$\delta_i := \delta_{a_i}, \quad \delta_{i_1 \dots i_N} := \delta_{a_{i_1}} \otimes \dots \otimes \delta_{a_{i_N}} \quad (2.1)$$

for $a_i \in X$ being a single point in the finite state space and $(a_{i_1}, \dots, a_{i_N})$ being an element of the product space X^N .

As announced in the Introduction, we will now take a closer look at the set of admissible trial states of problem (1.1), i.e., the set

$$\mathcal{P}_{\text{sym}, \bar{\lambda}}(X^N) := \{\gamma \in \mathcal{P}_{\text{sym}}(X^N) : \gamma \mapsto \bar{\lambda}\}. \quad (2.2)$$

From this point on, we will refer to the elements of this set as *symmetric Kantorovich couplings*. The set $\mathcal{P}_{\text{sym}, \bar{\lambda}}(X^N)$ will be called (*symmetric*) *Kantorovich polytope for N marginals and ℓ states*. As within this paper we focus our attention on the symmetric case, the term symmetric will be dropped from time to time. It is easy to see that, as a result of the linearity of the marginal constraint and the finiteness of the state space X , $\mathcal{P}_{\text{sym}, \bar{\lambda}}(X^N)$ is a compact and convex set in \mathbb{R}^{ℓ^N} and therefore by Minkowski's theorem (see, e.g., [23]) the convex hull of its extreme points.

Recall the following basic definitions and notions of convexity (see, e.g., [23, 33]). For $y_1, \dots, y_n \in \mathbb{R}^m$ and $\lambda_1, \dots, \lambda_n \geq 0$ such that $\sum_{i=1}^n \lambda_i = 1$

$$\lambda_1 y_1 + \dots + \lambda_n y_n = \sum_{i=1}^n \lambda_i y_i$$

is called a *convex combination of the points y_1, \dots, y_n* . A subset $K \subseteq \mathbb{R}^m$ is called *convex* if for each finite selection of points in K each possible convex combination of these points is again contained in K . For a subset $V \subseteq \mathbb{R}^m$ the *convex hull of V* , denoted as

$$\text{conv}(V),$$

corresponds to the set of all possible convex combinations of a finite selection of points in V . Obviously a set $K \subseteq \mathbb{R}^m$ is convex if and only if it is equal to its convex hull. Finally

an element k of the convex set $K \subseteq \mathbb{R}^m$ is called an *extreme point* if $k = \lambda_1 y_1 + \lambda_2 y_2$ for some $y_1, y_2 \in K$ and $\lambda_1, \lambda_2 > 0$ such that $\lambda_1 + \lambda_2 = 1$ implies $y_1 = k = y_2$. For a considered convex set K the set of extreme points will from now on be denoted as $\text{ext}(K)$.

As $\mathcal{P}_{\text{sym}, \bar{\lambda}}(X^N)$ is equal to the convex hull of its extreme points, we can use the extreme points to describe the convex structure of the set of symmetric Kantorovich couplings. Now it follows by a simple contradiction argument that for any given linear objective function there is always an optimizer that is an extreme point. Moreover, in our setting of finite states spaces, for any extreme point γ^* there is a function $c : X^N \rightarrow \mathbb{R}$ such that

$$\int_{X^N} c(x_1, \dots, x_N) d\gamma(x_1, \dots, x_N) > \int_{X^N} c(x_1, \dots, x_N) d\gamma^*(x_1, \dots, x_N) \quad \text{for any } \gamma \in \mathcal{P}_{\text{sym}, \bar{\lambda}}(X^N), \quad (2.3)$$

i.e., there is a cost function such that γ^* is the unique optimizer of the corresponding optimal transport problem. This is a result of the fact that $\mathcal{P}_{\text{sym}, \bar{\lambda}}(X^N)$ is a bounded polyhedron, i.e., a polytope, of finite dimension and therefore only possesses finitely many extreme points each of whom is itself an exposed point (see, e.g., [33]), i.e., a point in the set $\mathcal{P}_{\text{sym}, \bar{\lambda}}(X^N)$ that fulfills (2.3) for some cost function $c : X^N \rightarrow \mathbb{R}$. As for any cost function $c : X^N \rightarrow \mathbb{R}$ there is always an optimizer that is an extreme point of $\mathcal{P}_{\text{sym}, \bar{\lambda}}(X^N)$ and vice versa for any extreme point γ^* of $\mathcal{P}_{\text{sym}, \bar{\lambda}}(X^N)$ there is a cost function $c : X^N \rightarrow \mathbb{R}$ such that γ^* is the unique optimizer, analyzing, how many of the extreme points of $\mathcal{P}_{\text{sym}, \bar{\lambda}}(X^N)$ are of Monge-type, seems to be the right approach to investigate the validity of Monge's approach. Recall that in the given setting a probability measure $\gamma \in \mathcal{P}_{\text{sym}, \bar{\lambda}}(X^N)$ is said to be of Monge-type or in Monge-form if there are N permutations $\tau_1, \dots, \tau_N : \{1, \dots, \ell\} \rightarrow \{1, \dots, \ell\}$ such that

$$\gamma = \sum_{i=1}^{\ell} \frac{1}{\ell} S \delta_{\tau_1(i) \tau_2(i) \dots \tau_N(i)},$$

where the *symmetrization operator* $S : \mathcal{P}(X^N) \rightarrow \mathcal{P}_{\text{sym}}(X^N)$ is defined by

$$(S\gamma)(A_1 \times \dots \times A_N) = \frac{1}{N!} \sum_{\sigma \in S_N} \gamma(A_{\sigma(1)} \times \dots \times A_{\sigma(N)}) \quad \text{for all } A_1, \dots, A_N \subseteq X \quad (2.4)$$

with S_N being the group of all permutations on the set $\{1, \dots, N\}$.

As in the given setting it is rather inconvenient and long-winded to check whether a given symmetric Kantorovich coupling is of Monge-type or not, we will derive in the following an alternative LP-formulation of problem (1.1), where Monge-states will correspond exactly to (rescaled) integer points in the corresponding polytope of admissible trial states. We start by taking a closer look at the convex geometry of the set of symmetric probability measures on the product space X^N .

Note that a probability measure $\gamma \in \mathcal{P}_{\text{sym}}(X^N)$ is an extreme point of $\mathcal{P}_{\text{sym}}(X^N)$ if and only if it is of the form

$$S \delta_{i_1 \dots i_N} \quad \text{for some } 1 \leq i_1 \leq \dots \leq i_N \leq \ell \quad (2.5)$$

(see [18]). Therefore symmetric Kantorovich couplings, which are of Monge-type, are an average of ℓ not necessarily distinct extremal symmetric probability measures on the product space X^N with respect to the uniform measure. Below we will elaborate further on this characterization of couplings in Monge-form, which will be the basis for identifying Monge-states with the (rescaled) integer points in a certain polytope.

From now on, we will denote the set of extremal symmetric probability measures, i.e., measures of the form (2.5), as E_{sym}^N . It was shown in [18] that E_{sym}^N contains $\binom{N+\ell-1}{N}$ elements.

As for each pair of these extreme points their support is disjoint, one can immediately deduce the following result.

Proposition 2.1. $\mathcal{P}_{\text{sym}}(X^N)$ is a simplex, i.e., the extremal symmetric probability measures on X^N are affinely independent.

Hence, for every $\gamma \in \mathcal{P}_{\text{sym}}(X^N)$ there is a unique way to represent γ as a convex combination of extremal symmetric probability measures on X^N , i.e., there is a unique non-negative coefficient vector $\alpha \in \mathbb{R}^{|E_{\text{sym}}^N|}$ fulfilling $\sum \alpha_{i_1 \dots i_N} = 1$ such that

$$\gamma = \sum_{1 \leq i_1 \leq \dots \leq i_N \leq \ell} \alpha_{i_1 \dots i_N} S\delta_{i_1 \dots i_N}. \quad (2.6)$$

As the extreme points of $\mathcal{P}_{\text{sym}}(X^N)$ can be parametrized using their one-point marginal, α can be interpreted as a probability measure on the set of these one-point marginals.

Given the k -point marginal map $M_k : \mathcal{P}(X^N) \rightarrow \mathcal{P}(X^k)$ for $1 \leq k \leq N-1$ with

$$(M_k \gamma)(A) := \gamma(A \times X^{N-k}) \text{ for all } A \subseteq X^k \quad (2.7)$$

for $\gamma \in \mathcal{P}(X^N)$, with the convention $M_N = id$, note that M_1 is a bijection from the set of extremal symmetric probability measures on X^N , i.e., measures of the form (2.5), to the set of $\frac{1}{N}$ -quantized probability measures

$$\mathcal{P}_{\frac{1}{N}}(X) := \left\{ \lambda \in \mathcal{P}(X) : \lambda(\{i\}) \in \left\{ 0, \frac{1}{N}, \dots, 1 \right\} \right\} \quad (2.8)$$

(see [18]). Hereby the one-point marginal of a measure of form (2.5) is an empirical measure of the indices (i_1, \dots, i_N) , it holds

$$M_1 S\delta_{i_1 \dots i_N} = \frac{1}{N} \sum_{j=1}^N \delta_{i_j}.$$

In the following $\psi_N : \mathcal{P}_{\frac{1}{N}}(X) \rightarrow E_{\text{sym}}^N$ will denote the corresponding inverse function.

This parametrization gives rise to the *coefficients-to-coupling map* $R : \mathcal{P}\left(\mathcal{P}_{\frac{1}{N}}(X)\right) \rightarrow \mathcal{P}_{\text{sym}}(X^N)$. It maps an arbitrary probability measure α on $\mathcal{P}_{\frac{1}{N}}(X)$, which, via the underlying parametrization, corresponds to the coefficients in the representation (2.6), to the corresponding coupling γ , i.e., in pedestrian notation

$$R\alpha = \sum_{\lambda \in \mathcal{P}_{\frac{1}{N}}(X)} \alpha_\lambda \psi_N(\lambda),$$

or more elegantly

$$R\alpha = \int_{\mathcal{P}_{\frac{1}{N}}(X)} \psi_N(\lambda) d\alpha(\lambda).$$

As $\mathcal{P}_{\text{sym}}(X^N)$ is a simplex, R is bijective. This enables us to establish the following isomorphic relationship between two alternative formulations of the set of symmetric Kantorovich couplings.

Lemma 2.2 (isomorphic relationship between couplings and coefficients). *The coefficients-to-coupling map R maps the polytope*

$$P_{\text{coef}} := \left\{ \alpha \in \mathbb{R}^{|E_{\text{sym}}^N|} : A\alpha = \bar{\lambda}, \alpha \geq 0 \right\} \quad (2.9)$$

linearly and bijectively to the set of symmetric Kantorovich couplings, i.e., $\mathcal{P}_{\text{sym}, \bar{\lambda}}(X^N)$ defined in (2.2). Here E_{sym}^N is the set of extremal symmetric probability measures on X^N and A is the matrix in $\mathbb{R}^{\ell \times |E_{\text{sym}}^N|}$, whose columns are given by the elements of $\mathcal{P}_{\frac{1}{N}}(X)$, i.e.,

$$A := \begin{pmatrix} \lambda_1^{(1)} & \lambda_1^{(2)} & \dots & \lambda_1^{(|E_{\text{sym}}^N|)} \\ \vdots & \vdots & & \vdots \\ \lambda_\ell^{(1)} & \lambda_\ell^{(2)} & \dots & \lambda_\ell^{(|E_{\text{sym}}^N|)} \end{pmatrix}. \quad (2.10)$$

The corresponding inverse map is also linear.

Proof. Linearity and injectivity of R as a map from P_{coef} to $\mathcal{P}_{\text{sym}, \bar{\lambda}}(X^N)$ is an immediate consequence of the linearity and injective of $R : \mathcal{P}\left(\mathcal{P}_{\frac{1}{N}}(X)\right) \rightarrow \mathcal{P}_{\text{sym}}(X^N)$ as introduced above. We further know that any $\gamma \in \mathcal{P}_{\text{sym}, \bar{\lambda}}(X^N)$ is an element of $\mathcal{P}_{\text{sym}}(X^N)$. Hence, applying the parametrization of extremal symmetric probability measures on X^N via their one-point marginals, there exist coefficients $\alpha \in \mathcal{P}\left(\mathcal{P}_{\frac{1}{N}}(X)\right)$, which are non-negative and whose entries sum to 1 such that

$$\gamma = \sum_{\lambda \in \mathcal{P}_{\frac{1}{N}}(X)} \alpha_\lambda \psi_N(\lambda) \quad (2.11)$$

and therefore $\gamma = R\alpha$ holds. Applying the linear marginal map M_1 to (2.11) yields the following.

$$\bar{\lambda} = \sum_{\lambda \in \mathcal{P}_{\frac{1}{N}}(X)} \alpha_\lambda \lambda$$

Therefore α corresponds to an element of P_{coef} . This implies surjectivity of the considered map R . Linearity of the corresponding inverse map is an immediate consequence of the fact that the extremal symmetric probability measures on X^N of the form (2.5) interpreted as vectors are linearly independent. \square

Now it is easy to see that the extreme points of P_{coef} correspond exactly to the extremal symmetric Kantorovich couplings, in the sense that R maps the corresponding sets of extreme points bijectively to each other. By standard arguments of polyhedral optimization the extreme points of P_{coef} have a sparse structure, i.e., any extreme point of P_{coef} can have

at most ℓ , that is the number of states in the finite state space X , non-zero entries (see, e.g., [3]). In [18] it was shown that this implies that any extremal Kantorovich coupling is a so called *Quasi-Monge state*, i.e., of the form

$$\sum_{\nu=1}^{\ell} \alpha_{\nu} S \delta_{T_1(a_{\nu})} \otimes \cdots \otimes \delta_{T_N(a_{\nu})}$$

for N maps $T_1, \dots, T_N : X \rightarrow X$ such that

$$\frac{1}{N} \sum_{k=1}^N T_k \# \alpha = \bar{\lambda}.$$

Here we renounce from using the shorthand notations (2.1) in order to make it easier to draw a comparison with Monge's approach (1.5)-(1.7). The ansatz space of Quasi-Monge states increases the number of unknowns only by $2 \cdot \ell$ compared to the class of symmetrized Monge states and as every extremal Kantorovich coupling is a Quasi-Monge state, this ansatz space always contains an optimal coupling, in contrast to Monge's approach. Note further that obviously every symmetrized Monge state is a Quasi-Monge state. For further reading on this sufficient low-dimensional enlargement of the class of symmetrized Monge states we refer the interested reader to [18]. There also a characterization of Monge states in the given setting was established. A probability measure on the product space X^N is a symmetrized Monge state if and only if it is a Quasi-Monge state all of whose site weights $\alpha_1, \dots, \alpha_{\ell}$ are equal to $\frac{1}{\ell}$. In summary, we get the following corollary.

Corollary 2.3. *Extremal symmetric Kantorovich couplings correspond exactly, via the coefficients-to-coupling map R , to the extreme points of P_{coef} . Any of these extreme points of P_{coef} is the coefficient vector of a coupling in Monge-form if and only if it is an integer vector scaled by the factor $\frac{1}{\ell}$.*

This corollary gives us a numerically-convenient way to compute the set of extremal Kantorovich couplings and check whether they are of Monge-form or not. In addition we also want to consider Monge's approach by itself. For this purpose we introduce the sets

$$\mathcal{P}_{\text{sym,Monge}}(X^N) := \{ \gamma \in \mathcal{P}_{\text{sym},\bar{\lambda}}(X^N) : \gamma \text{ is of Monge-form (1.5) - (1.7)} \} \quad (2.12)$$

and

$$\mathcal{P}_{\text{sym,Monge}}^{\text{conv}}(X^N) := \text{conv}(\mathcal{P}_{\text{sym,Monge}}(X^N)). \quad (2.13)$$

$\mathcal{P}_{\text{sym,Monge}}(X^N)$ is the set of all symmetrized Monge states. In the following we will refer to $\mathcal{P}_{\text{sym,Monge}}^{\text{conv}}(X^N)$ as the *(symmetric) Monge polytope for N marginals and ℓ states*. For simplicity we will once again drop the term symmetric from time to time. Note that if there exists an optimizer of Problem (1.1) which is an element of $\mathcal{P}_{\text{sym,Monge}}^{\text{conv}}(X^N)$ then there exists a Monge-type minimizer.

Having the explanations leading up to Corollary 2.3 in mind, it is easy to see that $\mathcal{P}_{\text{sym,Monge}}(X^N)$ corresponds to the (scaled by $\frac{1}{\ell}$) integer elements of P_{coef} . These can be for example determined by a simple enumeration of all the ordered choices of $N - 1$ permutations interpreted as coefficient vectors in P_{coef} . Checking which of these scaled integer coefficient vectors are

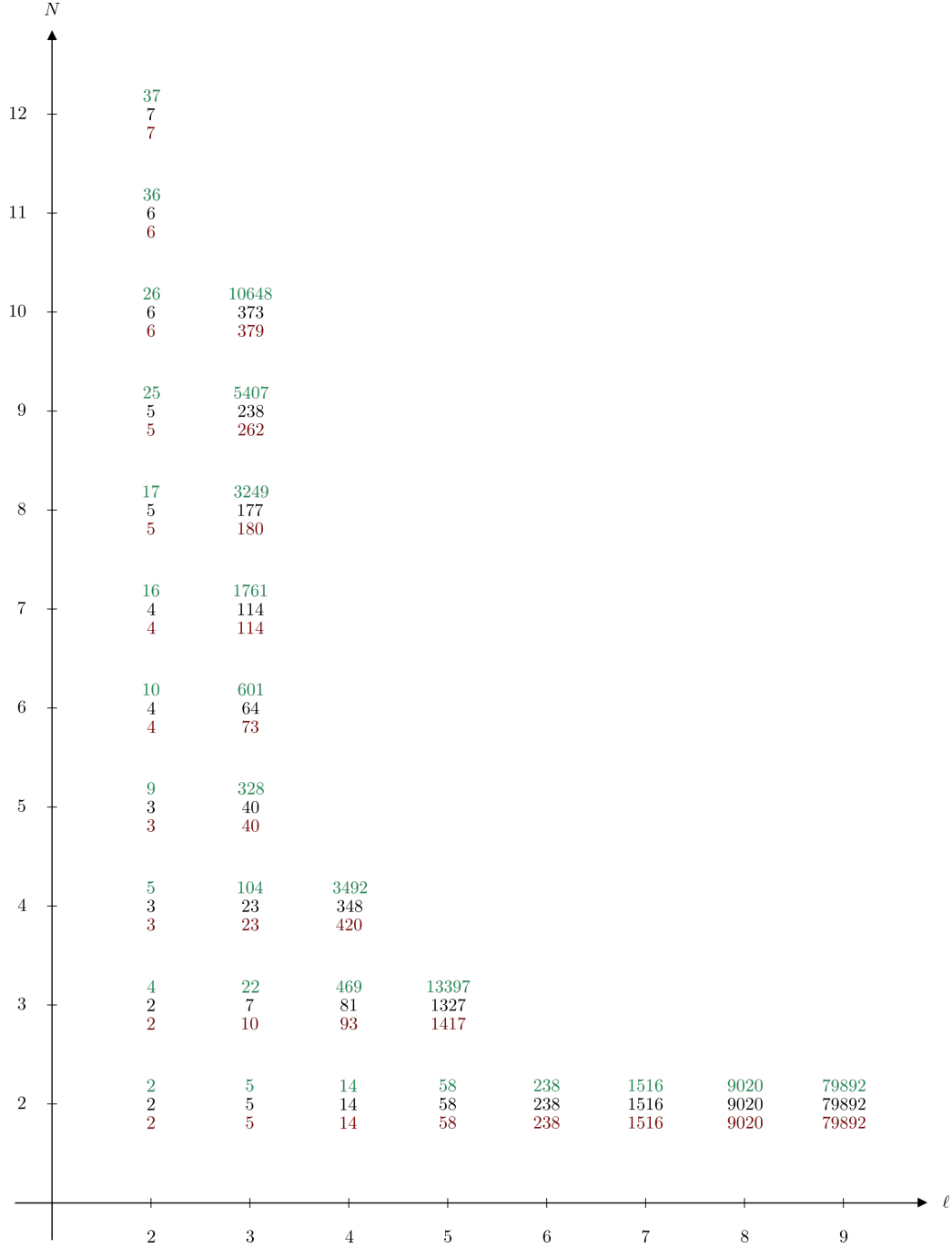


Figure 2: The number of extreme points of the symmetric Kantorovich polytope $\mathcal{P}_{\text{sym},\bar{\lambda}}(X^N)$ respectively of the symmetric Monge polytope $\mathcal{P}_{\text{sym},\text{Monge}}^{\text{conv}}(X^N)$ is given in green respectively red. The number of extreme points of $\mathcal{P}_{\text{sym},\bar{\lambda}}(X^N)$ that are of Monge-type (see (1.5)-(1.7)) is depicted in black. Here, as usual, N denotes the number of marginals and ℓ the number of states.

extremal with respect to the convex hull of them as a whole, gives us the extremal elements of $\mathcal{P}_{\text{sym},\text{Monge}}^{\text{conv}}(X^N)$.

The data in Figure 2 was computed using MATLAB [24] and polymake [31].

It was already mentioned above, that the extreme points of the polytope P_{coef} have a sparse structure. In more detail, a coefficient vector $\alpha \in P_{\text{coef}}$ is extremal with respect to the polytope P_{coef} if and only if its nonzero entries correspond to a selection of columns of A which are linearly independent (see, e.g., [3]). That is why, the complexity of computing the extreme points of P_{coef} , and their number, increases faster with the number of states than with the number of marginals. Suppose you are looking at a setting where the number of marginals is equal to the number of states. Then, on the one hand, increasing the number of marginals by 1 yields $\binom{2N}{N+1} - \binom{2N-1}{N}$ more columns in A . On the other hand, an increase in the number of states by 1 enlarges the number of columns of A by $\binom{2N}{N} - \binom{2N-1}{N}$. Elementary computations show that in the second case A has $\frac{1}{N+1}\binom{2N}{N}$ more columns than in the first case. Moreover, in contrast to an increase in the number of marginals, an increase in the number of states also increases the number of rows of A by 1. Therefore then up to $\ell + 1$ columns of A can be linearly independent. Hence, an increase in the number of states leads to a faster increasing (compared to an increase in the number of marginals) number of subsets of linearly independent columns of the constraint matrix A by yielding a steeper increase in the number of columns of A as well as by enlarging the dimension of the column space. Each of these subsets corresponds to an extreme point of P_{coef} .

Remark 2.4. This remark lists interpretations and observations regarding Figure 2.

- 1) In the case $N = 2$, Figure 2 shows that in the considered cases every extremal symmetric Kantorovich coupling is of Monge-type. In the given setting this means that every extreme point of $\mathcal{P}_{\text{sym},\bar{\lambda}}(X^N)$ is a symmetrized permutation matrix. It is easy to see, using the celebrated Birkhoff-von Neumann theorem [4, 36] as well as the linearity of the symmetrization operator S (2.4), that this holds true for an arbitrary number ℓ of states. Note, however, that not every symmetrized permutation matrix is an extreme point of $\mathcal{P}_{\text{sym},\bar{\lambda}}(X^N)$, but only those symmetrized Monge-states whose corresponding coefficient vectors select linearly independent columns of A .
- 2) In the case $\ell = 2$, the number of extremal symmetric Kantorovich couplings which are of Monge-type increases by 1 each time the marginal number is even. It is easy to prove that this pattern will continue. Firstly, note that, in the case $\ell = 2$, every symmetric Kantorovich coupling of Monge-type is an extreme point of $\mathcal{P}_{\text{sym},\bar{\lambda}}(X^N)$. This follows by a support-argument regarding the corresponding coefficient vectors. Secondly, we take a look at the symmetrized Monge-states in this setting. We assume the marginal vectors $\lambda^{(1)}, \dots, \lambda^{(N+1)}$ are sorted in the columns of A by the first component in decreasing order, i.e.,

$$A = \begin{pmatrix} 1 & \frac{N-1}{N} & \cdots & \frac{1}{N} & 0 \\ 0 & \frac{1}{N} & \cdots & \frac{N-1}{N} & 1 \end{pmatrix}.$$

Then the symmetric Kantorovich couplings of Monge-type are exactly those couplings with coefficient vectors

$$\alpha^{(j)} = \frac{1}{2}e^{(j)} + \frac{1}{2}e^{(N+1-j+1)}$$

for $j = 1, 2, \dots, \lceil \frac{N+1}{2} \rceil$, where $e^{(i)}$ is the i -th unit vector.

- 3) The setting of 3 marginals and 3 sites, i.e., $N = \ell = 3$ is the main focus in [16]. There interested readers can find the 22 extreme points of the symmetric Kantorovich polytope explicitly listed including the information which extremal elements are of Monge-type and which are not. This list also shows which pairs of permutations (identifying T_1 with the identity) correspond to an extremal symmetric Kantorovich coupling. [16] also visualizes these 22 extremal states as molecular packings, where one can identify irreducible packings with extreme points.

3 Classification of the Extreme Points of a Reduced Kantorovich Polytope

In Section 2, we achieved a better understanding of the optimal transport problem (1.1) by numerically analyzing the convex geometry of the set of admissible trial states, i.e., the set of symmetric Kantorovich couplings $\mathcal{P}_{\text{sym}, \bar{\lambda}}(X^N)$. Motivated by physical applications we assume from this point on that the given cost function has pairwise symmetric structure. Then the set of admissible trial states can be reduced by the linear map M_2 to a lower-dimensional polytope thereby decreasing the number of extremal states.

In more detail, we consider the optimal transport problem (1.1) with $c : X^N \rightarrow \mathbb{R}$ being a cost function with pairwise symmetric structure, i.e.,

$$c(x_1, \dots, x_N) = \sum_{1 \leq i < j \leq N} v(x_i, x_j) \text{ for all } (x_1, \dots, x_N) \in X^N, \quad (3.1)$$

where $v : X^2 \rightarrow \mathbb{R}$ is a symmetric pair-potential, i.e., $v(x, y) = v(y, x)$ for all $(x, y) \in X^2$. Then the objective function of (1.1) can be rewritten as

$$\int_{X^N} c(x_1, \dots, x_N) d\gamma(x_1, \dots, x_N) = \binom{N}{2} \int_{X^2} v(x, y) d(M_2\gamma)(x, y), \quad (3.2)$$

where $\gamma \in \mathcal{P}_{\text{sym}, \bar{\lambda}}(X^N)$ is an arbitrary symmetric Kantorovich coupling. This elementary reformulation was established in [17]. There also the concept of N -representability (see Definition 3.1) was introduced which we will use in the following to write the reduced set of admissible trial states in a compact manner.

Definition 3.1 (N -representability). *A probability measure $\mu \in \mathcal{P}(X^k)$ is called N -representable if there exists a symmetric probability measure γ on the product space X^N , i.e., $\gamma \in \mathcal{P}_{\text{sym}}(X^N)$, such that μ is its k -point marginal, i.e.,*

$$\mu = M_k\gamma. \quad (3.3)$$

Any such symmetric probability measure on X^N that fulfills (3.3) is then called a representing measure of μ . In the following the set of N -representable k -plans will be denoted by $\mathcal{P}_{N\text{-rep}}(X^k)$.

As we consider pairwise interactions, we will focus our attention on the set of N -representable 2-point measures, i.e., $\mathcal{P}_{N\text{-rep}}(X^2)$. Note, however, that cost functions c embodying k -particle interactions would give rise to a problem reformulation reducing the set of admissible trial states to a subset of $\mathcal{P}_{N\text{-rep}}(X^k)$. In the case $k = N$, c would be a symmetric cost which are, as mentioned in the introduction, 'dual' to the set of symmetric probability measures on the product space X^N . In the same manner, cost functions with symmetric pairwise structure have a dual relationship with the set of N -representable 2-plans.

By definition of N -representability (see Definition 3.1), the set of N -representable 2-point measures is the image of the set of symmetric probability measures on X^N under the map M_2 , defined in (2.7), i.e., $M_2(\mathcal{P}_{\text{sym}}(X^N)) = \mathcal{P}_{N\text{-rep}}(X^2)$. Combining this equality with (3.2) yields that (1.8) is an equivalent reformulation of the multi-marginal optimal transport problem (1.1) for a cost function with pairwise symmetric structure (3.1). Here (1.8) can also be written as

$$\min_{\mu \in \mathcal{P}_{N\text{-rep}, \bar{\lambda}}(X^2)} \int_{X^2} v(x, y) d\mu(x, y),$$

where $\mathcal{P}_{N\text{-rep}, \bar{\lambda}}(X^2)$ is the set of N -representable 2-plans having uniform marginal, i.e.,

$$\mathcal{P}_{N\text{-rep}, \bar{\lambda}}(X^2) := \{\mu \in \mathcal{P}_{N\text{-rep}}(X^2) : M_1(\mu) = \bar{\lambda}\}. \quad (3.4)$$

We will refer to the set $\mathcal{P}_{N\text{-rep}, \bar{\lambda}}(X^2)$ as *reduced Kantorovich polytope for N marginals and ℓ states*. The convex geometry of this set will be numerically analyzed in the following. Thereby the validity of Monge's approach in the given setting, i.e., symmetric multi-marginal optimal transport on finite state spaces with pairwise symmetric cost functions, will be tested.

We have seen above that under the assumption of pairwise symmetric cost functions the optimal transport problem (1.1), where the set of admissible trial states is given by the high-dimensional set $\mathcal{P}_{\text{sym}, \bar{\lambda}}(X^N)$, can be equivalently formulated as a minimization problem over the lower-dimensional set $\mathcal{P}_{N\text{-rep}, \bar{\lambda}}(X^2)$ (see (1.8)). The pairwise symmetric structure implies that any symmetric Kantorovich coupling influences the value of the objective function of problem (1.1) only through their respective two-point marginal (see (3.2)). The nature of this reformulation, applying the two-point marginal map M_2 on the set of symmetric Kantorovich couplings, however, entails that the new set of admissible trial states, i.e., the reduced Kantorovich polytope is only implicitly known. Only in the two-marginal ($N=2$) case the reduced Kantorovich polytope can be understood in a straightforward manner: It corresponds to the set of symmetric bistochastic matrices scaled by the factor $\frac{1}{\ell}$ (see Remark 3.5 1) below for further consideration of the two-marginal case). Hence, in the case $N = 2$, $\mathcal{P}_{N\text{-rep}, \bar{\lambda}}(X^2) = \mathcal{P}_{\text{sym}, \bar{\lambda}}(X^N)$ holds. For a better understanding of the multi-marginal ($N > 2$) case, we will in the following, as motivated, view the reduced Kantorovich polytope as the image of the set of symmetric Kantorovich couplings on X^N under the two-point marginal map, i.e.,

$$M_2(\mathcal{P}_{\text{sym}, \bar{\lambda}}(X^N)) = \mathcal{P}_{N\text{-rep}, \bar{\lambda}}(X^2). \quad (3.5)$$

As described in Section 2, $\mathcal{P}_{\text{sym}, \bar{\lambda}}(X^N)$ corresponds to the convex hull of its extreme points. Combining this fact with (3.5) and the linearity of M_2 yields that the reduced Kantorovich

polytope $\mathcal{P}_{N\text{-rep},\bar{\lambda}}(X^2)$ is equal to the convex hull of the two-point marginals of extremal symmetric Kantorovich couplings, i.e.,

$$\mathcal{P}_{N\text{-rep},\bar{\lambda}}(X^2) = \text{conv} \left(\{M_2\gamma : \gamma \text{ is an extreme point of } \mathcal{P}_{\text{sym},\bar{\lambda}}(X^N)\} \right). \quad (3.6)$$

The following proposition is an immediate consequence.

Proposition 3.2. *Any extreme point of the reduced Kantorovich polytope for N marginals and ℓ states is the two-point marginal of an extremal symmetric Kantorovich coupling.*

Now the question is whether or not M_2 represents a bijective relationship between the sets of extreme points of $\mathcal{P}_{\text{sym},\bar{\lambda}}(X^N)$ and $\mathcal{P}_{N\text{-rep},\bar{\lambda}}(X^2)$. The following remark sheds light on this issue applying the bijective relationship between $\mathcal{P}_{\text{sym},\bar{\lambda}}(X^N)$ and the polytope P_{coef} established in Lemma 2.2 and Corollary 2.3.

Remark 3.3. In Section 2 the extreme points of $\mathcal{P}_{\text{sym},\bar{\lambda}}(X^N)$, i.e., the set of admissible trial states of problem (1.1), are determined using the set's bijective relationship, captured in the coefficients-to-coupling map R introduced in Section 2, to the polytope P_{coef} . As explained above in more detail, the map R identifies any symmetric probability measure on X^N γ with a coefficient vector α , such that γ can be written as the respective convex combination of the extreme points of $\mathcal{P}_{\text{sym}}(X^N)$, i.e., (2.6) holds. These coefficients are unique due to the disjoint support of the extremal symmetric probability measures on X^N . It was proven in [18] that the two-point marginal map M_2 is a bijection between the sets of extreme points of $\mathcal{P}_{\text{sym}}(X^N)$ and $\mathcal{P}_{N\text{-rep}}(X^2)$, respectively. Due to the linearity of M_2 , given a coefficient vector α and a symmetric probability measure γ on X^N , such that $\gamma = R\alpha$, i.e., (2.6) holds true, then

$$M_2\gamma = \sum_{1 \leq i_1 \leq \dots \leq i_N \leq \ell} \alpha_{i_1, \dots, i_N} M_2 S \delta_{i_1, \dots, i_N}.$$

Only now, these coefficients α representing $M_2\gamma$ as a convex combination of the extreme points of the set of N -representable two-point measures may not be unique, rendering us unable to identify the extreme points of the reduced Kantorovich polytope with those of the coefficient-polytope P_{coef} .

The remark above illuminates why the extreme points of the set of symmetric Kantorovich couplings $\mathcal{P}_{\text{sym},\bar{\lambda}}(X^N)$ can not be identified with the extremal elements of the reduced Kantorovich polytope $\mathcal{P}_{N\text{-rep},\bar{\lambda}}(X^2)$ via M_2 . The two-point marginal map may for example map multiple extreme points of the set $\mathcal{P}_{\text{sym},\bar{\lambda}}(X^N)$ on a single point of $\mathcal{P}_{N\text{-rep},\bar{\lambda}}(X^2)$; this point may lie on a face or in the interior of $\mathcal{P}_{N\text{-rep},\bar{\lambda}}(X^2)$ (see [16] for an well-illustrated example).

Nevertheless, it was established in Proposition 3.2 that every extremal element of $\mathcal{P}_{N\text{-rep},\bar{\lambda}}(X^2)$ has a representing measure that is itself extremal with respect to $\mathcal{P}_{\text{sym},\bar{\lambda}}(X^N)$. The extreme points of this set of symmetric Kantorovich couplings were in Corollary 2.3 identified with the extreme points of P_{coef} . In combination with the in Remark 3.3 established connection between P_{coef} and $\mathcal{P}_{N\text{-rep},\bar{\lambda}}(X^2)$ this leads us to the following approach to determine the extremal elements of $\mathcal{P}_{N\text{-rep},\bar{\lambda}}(X^2)$:

1. We start by determining the extremal elements of P_{coef} . This was already done within the considerations of Section 2.

2. Every such extreme point is multiplied by the matrix $T \in \mathbb{R}^{\ell^2 \times |E_{\text{sym}}^N|}$ which is constructed as follows. The matrix A as defined in (2.10) lists all the elements of $\mathcal{P}_{\frac{1}{N}}(X)$ as columns. It was proven in [18] that for any element λ of $\mathcal{P}_{\frac{1}{N}}(X)$ the following holds:

$$M_2\psi_N(\lambda) = \frac{N}{N-1}\lambda \otimes \lambda - \frac{1}{N-1}(\text{id}, \text{id}) \# \lambda, \quad (3.7)$$

where the map ψ_N was introduced in Section 2. Note that it was further established in [18] that measures of form (3.7) for $\lambda \in \mathcal{P}_{\frac{1}{N}}(X)$ are exactly the extreme points of $\mathcal{P}_{N\text{-rep}}(X^2)$. Now we construct T by replacing any column λ of A with $M_2\psi_N(\lambda)$ as given in (3.7) where we canonically identify matrices with vectors by gluing columns together.

3. Finally we check which points of the form

$$T\alpha \text{ for } \alpha \in \text{ext}(P_{\text{coef}})$$

are extremal with respect to $\text{conv}(\{T\alpha : \alpha \in \text{ext}(P_{\text{coef}})\})$ and therefore by (3.6) with respect to $\mathcal{P}_{N\text{-rep}, \bar{\lambda}}(X^2)$.

Note that it is computationally more complex to determine the extremal elements of $\mathcal{P}_{N\text{-rep}, \bar{\lambda}}(X^2)$ than those of $\mathcal{P}_{\text{sym}, \bar{\lambda}}(X^N)$.

Now, we will incorporate Monge's approach in the reduced setting.

Definition 3.4. *An element of the reduced Kantorovich polytope for N marginals and ℓ states is said to be of Monge-type or in Monge-form if it has a representing measure that is of Monge-form (see (1.5)-(1.7)).*

This definition is consistent with our goal to check the validity of Monge's approach as any optimizer in Monge-form for problem (1.8) guarantees the existence of an optimizer in Monge-form for problem (1.1). The set of all elements of $\mathcal{P}_{N\text{-rep}, \bar{\lambda}}(X^2)$ which are in Monge-form will be denoted as $\mathcal{P}_{N\text{-rep}, \text{Monge}}(X^2)$, i.e.,

$$\mathcal{P}_{N\text{-rep}, \text{Monge}}(X^2) := \{M_2\gamma : \gamma \text{ is of Monge-type (1.5) - (1.7)}\}.$$

Analogously to (2.13) we introduce the *reduced Monge polytope for N marginals and ℓ states* $\mathcal{P}_{N\text{-rep}, \text{Monge}}^{\text{conv}}(X^2)$ as follows.

$$\mathcal{P}_{N\text{-rep}, \text{Monge}}^{\text{conv}}(X^2) := \text{conv}(\mathcal{P}_{N\text{-rep}, \text{Monge}}(X^2)) \quad (3.8)$$

The extremal elements of the reduced Monge polytope can be determined in the same manner as those of the reduced Kantorovich polytope (see the description of the procedure above). Starting point are now the extremal elements of the Monge polytope $\mathcal{P}_{\text{sym}, \text{Monge}}(X^N)$ interpreted as coefficient vectors.

Checking which of the extreme points of the reduced Kantorovich polytope $\mathcal{P}_{N\text{-rep}, \bar{\lambda}}(X^2)$ correspond to an extremal element of the reduced Monge polytope $\mathcal{P}_{N\text{-rep}, \text{Monge}}^{\text{conv}}(X^2)$ tells us which of the extreme points of $\mathcal{P}_{N\text{-rep}, \bar{\lambda}}(X^2)$ are of Monge-type.

The data in Figure 3 was computed using MATLAB [24] and polymake [31].

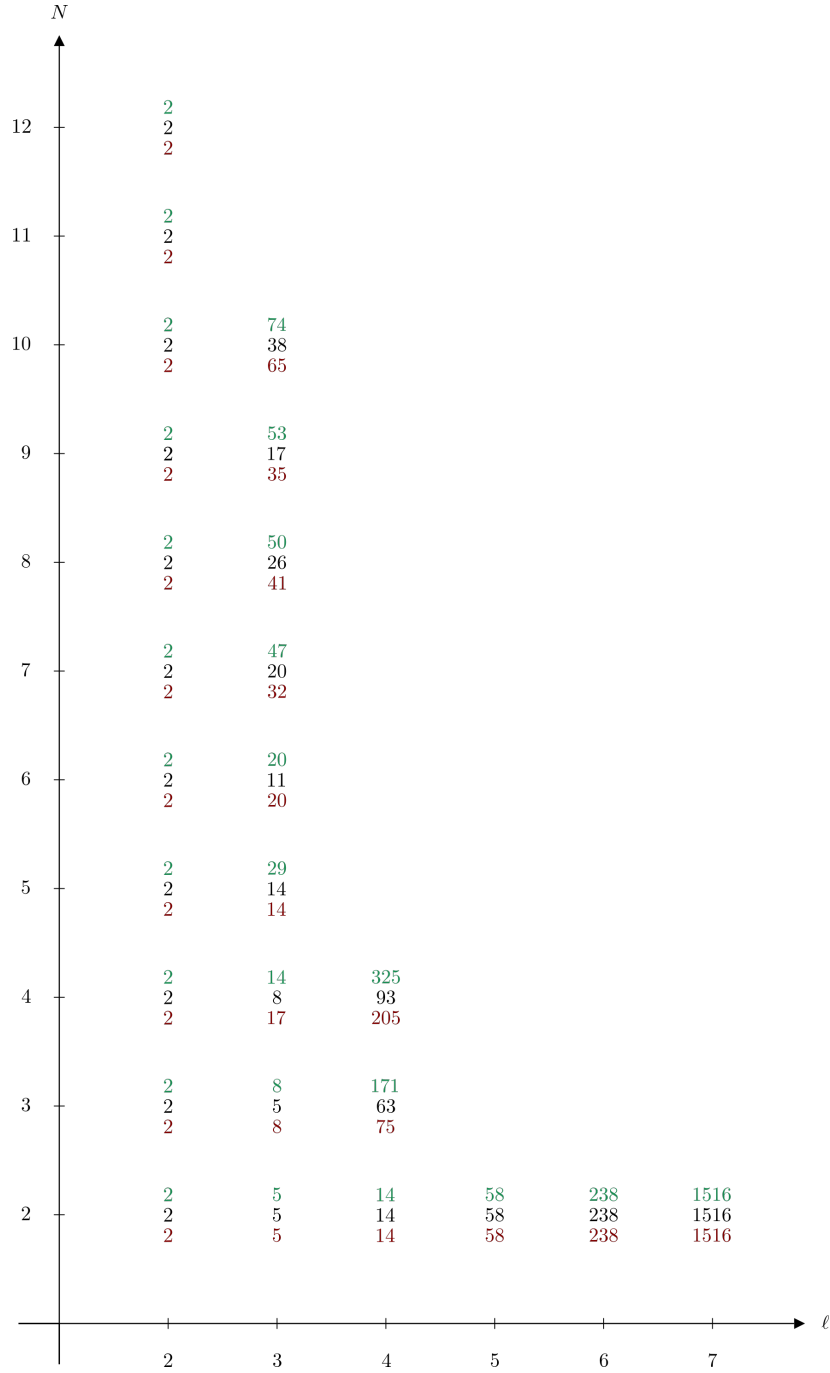


Figure 3: The number of extreme points of the reduced Kantorovich polytope $\mathcal{P}_{N\text{-rep},\bar{\lambda}}(X^2)$ respectively of the reduced Monge polytope $\mathcal{P}_{N\text{-rep},\text{Monge}}^{\text{conv}}(X^2)$ is given in green respectively red. The number of extreme points of $\mathcal{P}_{N\text{-rep},\bar{\lambda}}(X^2)$ that are of Monge-type (see Definition 3.4) is depicted in black. Here, as usual, N denotes the number of marginals and ℓ the number of states.

Remark 3.5. What follows are interpretations and observations regarding Figure 3.

- 1) Combining the convention $M_N = \text{id}$ with (3.5), it is obvious that the symmetric Kantorovich polytope for 2 marginals and ℓ states $\mathcal{P}_{\text{sym},\bar{\lambda}}(X^2)$ coincides with the reduced Kantorovich polytope for 2 marginals and ℓ states $\mathcal{P}_{2\text{-rep},\bar{\lambda}}(X^2)$. This fact was already mentioned above. It was established in Remark 2.4 that every extreme point of $\mathcal{P}_{\text{sym},\bar{\lambda}}(X^2)$ is a symmetrized permutation matrix, i.e., the image of a permutation matrix under the symmetrization operator (2.4). In the setting of 2 marginals, symmetrized permutation matrices exactly correspond to symmetrized Monge states. See Remark 2.4 for further considerations of the case $N = 2$.
- 2) In the case $\ell = 2$, Figure 3 depicts that in the considered cases, the reduced Kantorovich polytope $\mathcal{P}_{N\text{-rep},\bar{\lambda}}(X^2)$ has two extreme points both of which are in Monge-form. Hence, in any considered case the line segment $\mathcal{P}_{N\text{-rep},\bar{\lambda}}(X^2)$ coincides with the respective reduced Monge polytope $\mathcal{P}_{N\text{-rep},\text{Monge}}^{\text{conv}}(X^2)$.

One can prove by elementary arguments that this holds true for an arbitrary number of marginals N in the case of 2 sites. In a little more detail, considering the dimension of $\mathcal{P}_{N\text{-rep},\bar{\lambda}}(X^2)$ in the given case and parametrising the elements of $\mathcal{P}_{N\text{-rep},\bar{\lambda}}(X^2)$ by their off-diagonal element allows us to deduce that the two extreme points of $\mathcal{P}_{N\text{-rep},\bar{\lambda}}(X^2)$ are given by

$$\mu^{(1)} = M_2 \left(\frac{1}{2}\psi_N(\delta_1) + \frac{1}{2}\psi_N(\delta_2) \right) \quad (3.9)$$

$$\mu^{(2)} = \begin{cases} M_2 \left(\psi_N \left(\frac{1}{2}\delta_1 + \frac{1}{2}\delta_2 \right) \right) & \text{if } N \text{ is even} \\ M_2 \left(\frac{1}{2}\psi_N \left(\frac{N-1}{2N}\delta_1 + \frac{N+1}{2N}\delta_2 \right) + \frac{1}{2}\psi_N \left(\frac{N+1}{2N}\delta_1 + \frac{N-1}{2N}\delta_2 \right) \right) & \text{if } N \text{ is odd} \end{cases} \quad (3.10)$$

or in pedestrian notation,

$$\mu^{(1)} = \begin{pmatrix} \frac{1}{2} & 0 \\ 0 & \frac{1}{2} \end{pmatrix}$$

$$\mu^{(2)} = \begin{cases} \frac{1}{4(N-1)} \begin{pmatrix} N-2 & N \\ N & N-2 \end{pmatrix} & \text{if } N \text{ is even} \\ \frac{1}{4N} \begin{pmatrix} N-1 & N+1 \\ N+1 & N-1 \end{pmatrix} & \text{if } N \text{ is odd.} \end{cases}$$

As the coefficients in (3.9) and (3.10) are integer multiples of $\frac{1}{\ell}$ both extreme points are 2-point marginals of symmetric Kantorovich couplings in Monge-form and therefore they are themselves elements of the reduced Kantorovich polytope $\mathcal{P}_{N\text{-rep},\bar{\lambda}}(X^2)$ which are of Monge-type (see Definition 3.4). Note that $\mu^{(2)}$, which is of Monge-type and therefore describes a correlated or in other words deterministic state, converges for $N \rightarrow \infty$ to the independent measure $\lambda \otimes \lambda$ for $\lambda = \left(\frac{1}{2}\delta_1 + \frac{1}{2}\delta_2 \right)$.

These findings coincide with the results in [17], where a model problem of N particles on 2 sites was considered. There also the set of N -representable 2-plans $\mathcal{P}_{N\text{-rep}}(X^2)$ for X consisting of 2 distinct elements is illustrated. Imposing the here given marginal condition on these sets leads to the respective line segment $\mathcal{P}_{N\text{-rep},\bar{\lambda}}(X^2)$.

- 3) The case of 3 marginals and 3 sites, i.e., $N = \ell = 3$, is a minimal example of a point in the grid, both with respect to the sum of both parameters $N + \ell$ and with respect to the minimum of both parameters $\min\{N, \ell\}$, such that not every extremal element of the reduced Kantorovich polytope $\mathcal{P}_{N\text{-rep}, \bar{\lambda}}(X^2)$ is of Monge-type. In the considered case $\mathcal{P}_{N\text{-rep}, \bar{\lambda}}(X^2)$ has 8 extreme points 5 of which are in Monge-form. By extension 3 of them are not. They are given by

$$\frac{1}{2}M_2(S\delta_{112}) + \frac{1}{2}M_2(S\delta_{233}) \quad (3.11)$$

and the two states one generates by imposing the role of the second site on the first and third site respectively. (3.11) is the unique optimizer of an optimal transport problem stated in [16]. This problem corresponds to a molecular packing problem. See [16] for further reading.

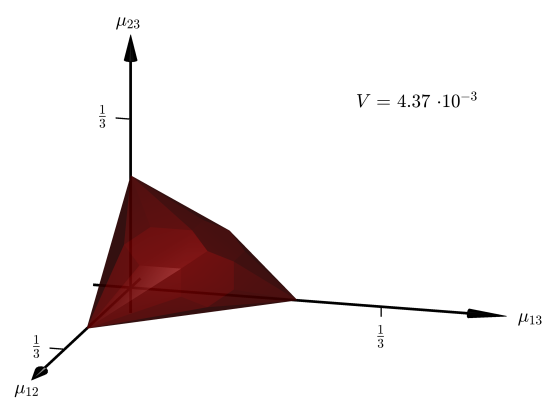
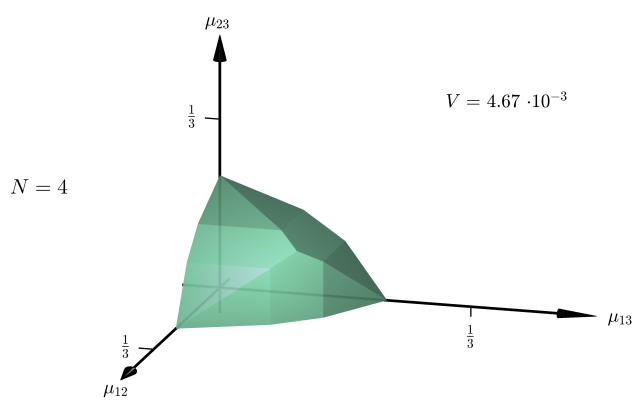
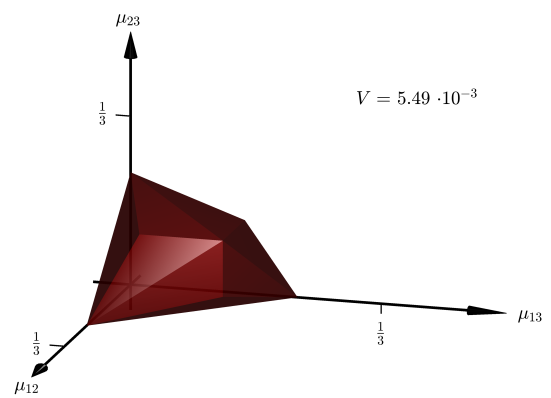
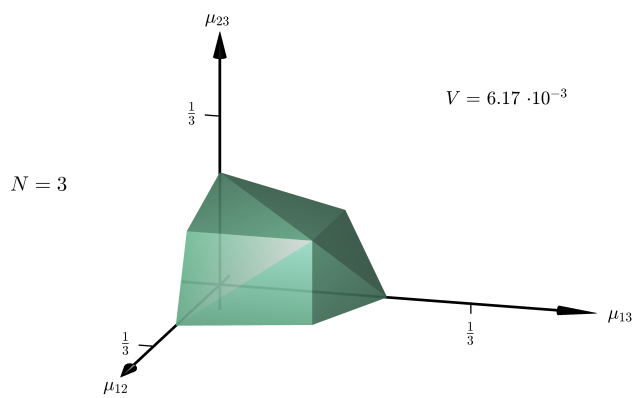
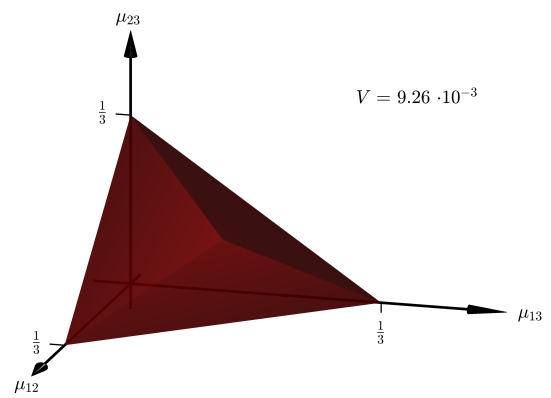
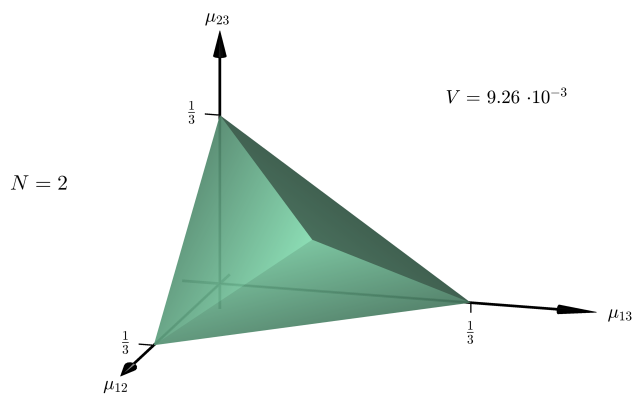
4 A Model Problem: Optimal Couplings of N marginals on 3 sites for pairwise costs

In the following, we focus our attention on symmetric multi-marginal optimal transport problems (1.1) on 3 sites, i.e., $X = \{a_1, a_2, a_3\}$. As in Section 3, we only consider pairwise symmetric costs and therefore are able to reformulate (1.1) as the lower-dimensional problem (1.8). In particular, the reduced Kantorovich polytope for N marginals and 3 states corresponds to the respective set of admissible trial states. It is easy to see that in the given setting these polytopes are three-dimensional. As by extension the reduced Monge polytope is at most three-dimensional, we are able to visually compare both approaches.

The following visualizations in Figure 4 were generated by extending the above explained calculations and routines in MATLAB [24] and polymake [31].

Note that by definition the reduced Monge polytope is always contained in the reduced Kantorovich polytope independently of the number of marginals N and the number of sites ℓ . Some of the extreme points of the reduced Monge polytope are also extremal with respect to the reduced Kantorovich polytope and some lie on faces or in the interior of the latter (see Figure 3 for specific numbers).

In the setting of $\ell = 3$ sites, the numerical analysis of the reduced setting discussed in Section 3 yields that in the case of $N = 2, 3, \dots, 9$ and 10 marginals there are always 5 prominent extreme points of the reduced Kantorovich polytope that are of Monge-type. This is also indicated by Figure 1 as well as Figure 4. In the illustrations they can be identified with the four extreme points on the co-ordinate axes, including the origin, as well as the 'peak' in the front of the polytopes. In formulas these extreme points can be written as depicted in Table 1.



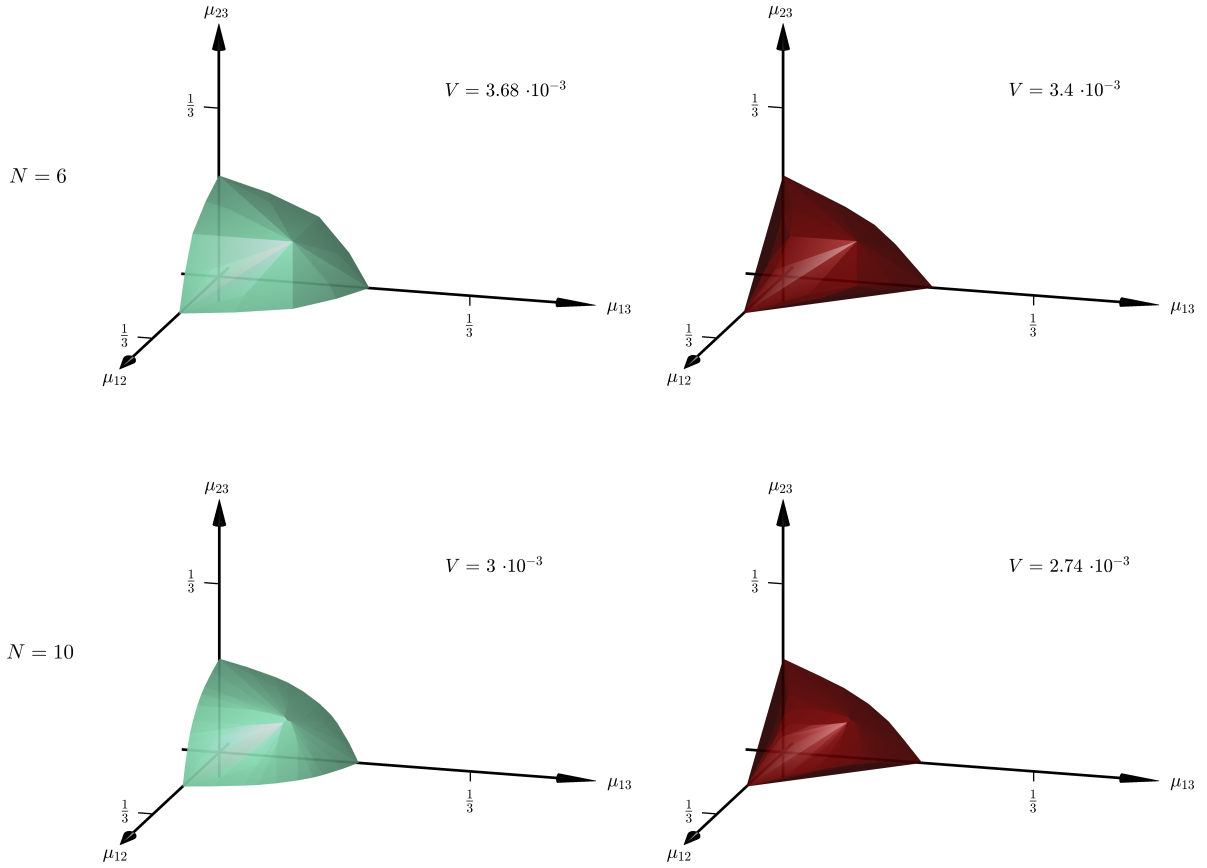


Figure 4: The reduced Kantorovich respectively Monge polytope for N marginals and 3 states is visualized for $N = 2, 3, 4, 6$ and 10 in green respectively red. The plots are arranged in ascending order with respect to N . The elements $(\mu_{ij})_{i,j=1}^3$ of the polytopes are parametrized by their off-diagonal entries μ_{12}, μ_{13} and μ_{23} . In the case of three marginals the reduced polytopes were initially depicted in [16]. V indicates the volume of the corresponding polytope. The volumetric ratio, reduced Monge polytope to reduced Kantorovich polytope, is depicted in Figure 6.

Nomenclature		Abstract Notation	Matrix Notation
$EA^{(N)}$	$EA^{(N)}$	$\frac{1}{3}M_2\psi_N(\delta_1)$ $+\frac{1}{3}M_2\psi_N(\delta_2)$ $+\frac{1}{3}M_2\psi_N(\delta_3)$	$\begin{pmatrix} \frac{1}{3} & 0 & 0 \\ 0 & \frac{1}{3} & 0 \\ 0 & 0 & \frac{1}{3} \end{pmatrix}$
$ER^{(N)}$	$ER^{(3m)}$	$M_2\psi_N(\frac{1}{3}\delta_1 + \frac{1}{3}\delta_2 + \frac{1}{3}\delta_3)$	$\begin{pmatrix} \frac{N-3}{9(N-1)} & \frac{N}{9(N-1)} & \frac{N}{9(N-1)} \\ \frac{N}{9(N-1)} & \frac{N-3}{9(N-1)} & \frac{N}{9(N-1)} \\ \frac{N}{9(N-1)} & \frac{N}{9(N-1)} & \frac{N-3}{9(N-1)} \end{pmatrix}$
	$ER^{(3m+1)}$	$\frac{1}{3}M_2\psi_N(\frac{m}{N}\delta_1 + \frac{m}{N}\delta_2 + \frac{m+1}{N}\delta_3)$ $+\frac{1}{3}M_2\psi_N(\frac{m}{N}\delta_1 + \frac{m+1}{N}\delta_2 + \frac{m}{N}\delta_3)$ $+\frac{1}{3}M_2\psi_N(\frac{m+1}{N}\delta_1 + \frac{m}{N}\delta_2 + \frac{m}{N}\delta_3)$	$\begin{pmatrix} \frac{N-2}{9N} & \frac{N+1}{9N} & \frac{N+1}{9N} \\ \frac{N+1}{9N} & \frac{N-2}{9N} & \frac{N+1}{9N} \\ \frac{N+1}{9N} & \frac{N+1}{9N} & \frac{N-2}{9N} \end{pmatrix}$
	$ER^{(3m+2)}$	$\frac{1}{3}M_2\psi_N(\frac{m}{N}\delta_1 + \frac{m+1}{N}\delta_2 + \frac{m+1}{N}\delta_3)$ $+\frac{1}{3}M_2\psi_N(\frac{m+1}{N}\delta_1 + \frac{m}{N}\delta_2 + \frac{m+1}{N}\delta_3)$ $+\frac{1}{3}M_2\psi_N(\frac{m+1}{N}\delta_1 + \frac{m+1}{N}\delta_2 + \frac{m}{N}\delta_3)$	$\begin{pmatrix} \frac{N-2}{9N} & \frac{N+1}{9N} & \frac{N+1}{9N} \\ \frac{N+1}{9N} & \frac{N-2}{9N} & \frac{N+1}{9N} \\ \frac{N+1}{9N} & \frac{N+1}{9N} & \frac{N-2}{9N} \end{pmatrix}$
$E12^{(N)}$	$E12^{(2m)}$	$\frac{2}{3}M_2\psi_N(\frac{1}{2}\delta_1 + \frac{1}{2}\delta_2) + \frac{1}{3}M_2\psi_N\delta_3$	$\begin{pmatrix} \frac{N-2}{6(N-1)} & \frac{N}{6(N-1)} & 0 \\ \frac{N}{6(N-1)} & \frac{N-2}{6(N-1)} & 0 \\ 0 & 0 & \frac{1}{3} \end{pmatrix}$
	$E12^{(2m+1)}$	$\frac{1}{3}M_2\psi_N(\frac{N-1}{2N}\delta_1 + \frac{N+1}{2N}\delta_2)$ $+\frac{1}{3}M_2\psi_N(\frac{N+1}{2N}\delta_1 + \frac{N-1}{2N}\delta_2)$ $+\frac{1}{3}M_2\psi_N(\delta_3)$	$\begin{pmatrix} \frac{N-1}{6N} & \frac{N+1}{6N} & 0 \\ \frac{N+1}{6N} & \frac{N-1}{6N} & 0 \\ 0 & 0 & \frac{1}{3} \end{pmatrix}$

Table 1: The extreme points $EA^{(N)}$, $ER^{(N)}$ and $E12^{(N)}$ of the reduced Kantorovich polytope are depicted in abstract and matrix notation. Hereby N corresponds to the number of marginals and $m \in \mathbb{N}_0$ is a non-negative integer, allowing us to distinguish between the various cases regarding N . As all the coefficients in the 'Abstract Notation'-column are integer multiples of $\frac{1}{3}$, these extreme points are of Monge-type.

In Figure 4, $EA^{(N)}$ corresponds to the origin, $ER^{(N)}$ to the 'peak' and $E12^{(N)}$ to the non-origin extreme point on the μ_{12} -axis. $E12^{(N)}$ assumes an exemplary role in Table 1. The corresponding extreme points on the μ_{13} - respectively μ_{23} -axis can be expressed analogously in abstract as well as matrix notation and will be denoted by $E13^{(N)}$ respectively $E23^{(N)}$.

So far we know by numerical analysis that $EA^{(N)}$, $ER^{(N)}$, $E12^{(N)}$, $E13^{(N)}$ and $E23^{(N)}$ are extreme points of the reduced Kantorovich polytope $\mathcal{P}_{N\text{-rep},\bar{\lambda}}(X^2)$ in the cases of $N = 2, 3, \dots, 9$ and 10 marginals. One can prove that this holds true for a general number $N \geq 2$ of marginals. For $E12^{(N)}$, $E13^{(N)}$ and $E23^{(N)}$ one can show this by following the same approach taken in Remark 3.5 2). In case of $EA^{(N)}$ and $ER^{(N)}$ it is an immediate consequence of Theorem 4.1. In the following $d : X \times X \rightarrow \mathbb{R}$ will denote the discrete metric defined by

$$d(x, y) := \begin{cases} 1 & \text{if } x \neq y \\ 0 & \text{if } x = y. \end{cases}$$

Theorem 4.1. *We consider the reduced multi-marginal optimal transport problem (1.8) for $N \geq 2$ marginals and $\ell = 3$ sites.*

a) *For the attractive cost function $d : X \times X \rightarrow \mathbb{R}$ the unique minimizer is given by $EA^{(N)}$.*

b) For the repulsive cost function $c_R : X \times X \rightarrow \mathbb{R}$ given by

$$c_R(x, y) := \begin{cases} \frac{1}{d(x, y)} & \text{if } x \neq y \\ B & \text{if } x = y \end{cases} \quad (4.1)$$

for some constant $B > 1$, the unique minimizer is given by $ER^{(N)}$.

Proof. In the following the elements of the reduced Kantorovich polytope will always be interpreted as matrices. Along those lines D respectively CR corresponds to the matrix notation of d respectively c_R , i.e., $D_{ij} := d(a_i, a_j)$ respectively $CR_{ij} := c_R(a_i, a_j)$ for $i, j \in \{1, 2, \dots, \ell\}$, and $\langle \cdot, \cdot \rangle$ denotes the standard matrix scalar product.

- a) Note that by non-negativity of the cost function d the objective value of an arbitrary admissible state $\mu \in \mathcal{P}_{N\text{-rep}, \bar{\lambda}}(X^2)$ is non-negative, i.e., $\langle D, \mu \rangle \geq 0$. As $EA^{(N)}$ is admissible and yields an objective value of 0, i.e., $\langle D, EA^{(N)} \rangle = 0$, it is an optimizer of the corresponding problem (1.8). Positivity of D in its off-diagonal entries and the marginal constraint ensure that $EA^{(N)}$ is the unique optimizer.
- b) To prove the second assertion, we drop the marginal constraint in a reformulated version of the considered problem (1.8) and calculate the extremal elements of $\mathcal{P}_{N\text{-rep}}(X^2)$, which solve the new optimization problem. There will be a unique convex combination of the optimal extreme points of $\mathcal{P}_{N\text{-rep}}(X^2)$, namely $ER^{(N)}$, that lies in $\mathcal{P}_{N\text{-rep}, \bar{\lambda}}(X^2)$. This state then corresponds to the unique minimizer of problem (1.8).

We consider the problem

$$\min_{\mu \in \mathcal{P}_{N\text{-rep}, \bar{\lambda}}(X^2)} \langle CR, \mu \rangle. \quad (4.2)$$

Subsequently changing the objective function to $\langle CR - \mathbb{1}, \cdot \rangle$, where all the entries of $\mathbb{1} \in \mathbb{R}^{3 \times 3}$ are given by 1, and plugging in the marginal constraint allows us to reformulate (4.2) as follows

$$\max_{\mu \in \mathcal{P}_{N\text{-rep}, \bar{\lambda}}(X^2)} \mu_{12} + \mu_{13} + \mu_{23}. \quad (4.3)$$

By dropping the marginal constraint, further restricting the admissible set to the extreme points (3.7) of $\mathcal{P}_{N\text{-rep}}(X^2)$ and rescaling the new admissible set by N^2 leads to the new optimization problem

$$\max_{\lambda \in N\mathcal{P}_{\frac{1}{N}}(X)} \lambda_1 \lambda_2 + \lambda_1 \lambda_3 + \lambda_2 \lambda_3 = \lambda_1 \lambda_2 + (N - \lambda_3) \lambda_3. \quad (4.4)$$

Assuming $(\lambda_1^*, \lambda_2^*, \lambda_3^*)$ is an optimizer of problem (4.4), then elementary calculations show that $(\lambda_1^*, \lambda_2^*)$ fulfills

$$(\lambda_1^*, \lambda_2^*) \in \begin{cases} \left\{ \left(\frac{r}{2}, \frac{r}{2} \right) \right\} & \text{if } r \text{ is even} \\ \left\{ \left(\frac{r-1}{2}, \frac{r+1}{2} \right), \left(\frac{r+1}{2}, \frac{r-1}{2} \right) \right\} & \text{if } r \text{ is odd,} \end{cases} \quad (4.5)$$

where $r := N - \lambda_3^*$. Otherwise $(\lambda_1^*, \lambda_2^*, \lambda_3^*)$ would not be optimal. Note that (4.4) always admits a maximizer as $\mathcal{P}_{\frac{1}{N}}(X)$ is finite.

This allows us to identify problem (4.4) with the one-parameter optimization problem

$$\max \left\{ \max_{r \in 2\mathbb{N}_0, r \leq N} -\frac{3}{4}r^2 + Nr, \max_{r \in 2\mathbb{N}_0+1, r \leq N} -\frac{3}{4}r^2 + Nr - \frac{1}{4} \right\}. \quad (4.6)$$

Elementary calculations reveal that $r \in \{0, 1, \dots, N\}$ is optimal regarding (4.6) if and only if

$$r \in \begin{cases} \{2m\} & \text{if } N = 3m \text{ for } m \in \mathbb{N}_0 \\ \{2m, 2m + 1\} & \text{if } N = 3m + 1 \text{ for } m \in \mathbb{N}_0 \\ \{2m + 1, 2m + 2\} & \text{if } N = 3m + 2 \text{ for } m \in \mathbb{N}_0. \end{cases}$$

It immediately follows that $\lambda \in N\mathcal{P}_{\frac{1}{N}}(X)$ is optimal with respect to problem (4.4) if and only if

$$\lambda \in \begin{cases} N \left\{ \left(\frac{m}{N}, \frac{m}{N}, \frac{m}{N} \right) \right\} & \text{if } N = 3m \text{ for } m \in \mathbb{N}_0 \\ N \left\{ \left(\frac{m}{N}, \frac{m}{N}, \frac{m+1}{N} \right), \left(\frac{m}{N}, \frac{m+1}{N}, \frac{m}{N} \right), \left(\frac{m+1}{N}, \frac{m}{N}, \frac{m}{N} \right) \right\} & \text{if } N = 3m + 1 \text{ for } m \in \mathbb{N}_0 \\ N \left\{ \left(\frac{m}{N}, \frac{m+1}{N}, \frac{m+1}{N} \right), \left(\frac{m+1}{N}, \frac{m}{N}, \frac{m+1}{N} \right), \left(\frac{m+1}{N}, \frac{m+1}{N}, \frac{m}{N} \right) \right\} & \text{if } N = 3m + 2 \text{ for } m \in \mathbb{N}_0. \end{cases} \quad (4.7)$$

Recall that (3.7) allows us (after dropping the factor N in (4.7)) to identify the given maximizers with exactly those extremal elements of $\mathcal{P}_{N\text{-rep}}(X^2)$ that maximize the sum of their off-diagonal entries. As by Minkowski's theorem any element of $\mathcal{P}_{N\text{-rep}, \bar{\lambda}}(X^2)$ can be written as convex combination of the extreme points of $\mathcal{P}_{N\text{-rep}}(X^2)$ and in any of the considered cases in (4.7) there are unique coefficients given by

$$\begin{aligned} \alpha_1 &= 1 & \text{if } N = 3m \text{ for } m \in \mathbb{N}_0 \\ \alpha_1 = \alpha_2 = \alpha_3 &= \frac{1}{3} & \text{else} \end{aligned}$$

that allow us to write $\bar{\lambda}$ as a convex combination of the respective optimizers in (4.7), it is easy to see that $ER^{(N)}$ as defined in Table 1 is the unique optimizer of (4.3) and thereby (4.2) for any $N \geq 2$. □

Remark 4.2. It is an immediate consequence of Theorem 4.1 that

$$\gamma_{GS} := \frac{1}{3}S\delta_{11\dots 1} + \frac{1}{3}S\delta_{22\dots 2} + \frac{1}{3}S\delta_{33\dots 3}$$

respectively

$$\gamma_C := \frac{1}{3}S\delta_{1\tau(1)\dots\tau(N-1)(1)} + \frac{1}{3}S\delta_{2\tau(2)\dots\tau(N-1)(2)} + \frac{1}{3}S\delta_{3\tau(3)\dots\tau(N-1)(3)},$$

where $\tau : \{1, 2, 3\} \rightarrow \{1, 2, 3\}$ is the cyclic permutation defined by $\tau(1) = 2$, $\tau(2) = 3$, $\tau(3) = 1$ and $\tau^{(i)}$ denotes the i -th composition of τ with itself, is a solution to the optimal transport problem (1.1) for the Gangbo-Świąch cost function $c_{GS} : X^N \rightarrow \mathbb{R}$ defined by

$$c_{GS}(x_1, \dots, x_N) := \sum_{1 \leq i < j \leq N} d(x_i, x_j) \quad (4.8)$$

respectively the Coulomb cost function $c_C : X^N \rightarrow \mathbb{R}$ defined by

$$c_C(x_1, \dots, x_N) := \sum_{1 \leq i < j \leq N} c_R(x_i, x_j).$$

Here (4.8) is a discretization of the pair-cost considered in [20]. Note that one could replace $d(\cdot, \cdot)$ in (4.8) with $d(\cdot, \cdot)^p$ for any $p > 1$ without changing c_{GS} .

Next, we examine the behavior of the sequences $(EA^{(N)})_{N \geq 2}$, $(ER^{(N)})_{N \geq 2}$, $(E12^{(N)})_{N \geq 2}$, $(E13^{(N)})_{N \geq 2}$ and $(E23^{(N)})_{N \geq 2}$ for N tending to ∞ . Taking a look at the right column in Table 1, it is easy to see that the following holds true.

$$EA^{(N)} \xrightarrow{N \rightarrow \infty} \begin{pmatrix} \frac{1}{3} & 0 & 0 \\ 0 & \frac{1}{3} & 0 \\ 0 & 0 & \frac{1}{3} \end{pmatrix} =: EA^{(\infty)}, ER^{(N)} \xrightarrow{N \rightarrow \infty} \begin{pmatrix} \frac{1}{9} & \frac{1}{9} & \frac{1}{9} \\ \frac{1}{9} & \frac{1}{9} & \frac{1}{9} \\ \frac{1}{9} & \frac{1}{9} & \frac{1}{9} \end{pmatrix} =: ER^{(\infty)},$$

$$E12^{(N)} \xrightarrow{N \rightarrow \infty} \begin{pmatrix} \frac{1}{6} & \frac{1}{6} & 0 \\ \frac{1}{6} & \frac{1}{6} & 0 \\ 0 & 0 & \frac{1}{3} \end{pmatrix} =: E12^{(\infty)}$$

Here $E12^{(\infty)}$ assumes again an exemplary role and $E13^{(\infty)}$ as well as $E23^{(\infty)}$ are defined in an analogous manner. One can express these 'limit extreme points' in a more probabilistic manner $EA^{(\infty)} = \frac{1}{3}\delta_{11} + \frac{1}{3}\delta_{22} + \frac{1}{3}\delta_{33}$, $ER^{(\infty)} = (\frac{1}{3}\delta_1 + \frac{1}{3}\delta_2 + \frac{1}{3}\delta_3) \otimes (\frac{1}{3}\delta_1 + \frac{1}{3}\delta_2 + \frac{1}{3}\delta_3)$ as well as $E12^{(\infty)} = \frac{2}{3}(\frac{1}{2}\delta_1 + \frac{1}{2}\delta_2) \otimes (\frac{1}{2}\delta_1 + \frac{1}{2}\delta_2) + \frac{1}{3}\delta_3$ corresponding to the 'Abstract Notation'-column in Table 1 via (3.7).

In the following, $\mathcal{D}_{\infty\text{-rep},\bar{\lambda}}$ will denote the convex hull of these 'limit extreme points', i.e.,

$$\mathcal{D}_{\infty\text{-rep},\bar{\lambda}} = \text{conv}(\{EA^{(\infty)}, ER^{(\infty)}, E12^{(\infty)}, E13^{(\infty)}, E23^{(\infty)}\}). \quad (4.9)$$

For an illustration of $\mathcal{D}_{\infty\text{-rep},\bar{\lambda}}$ see Figure 5.

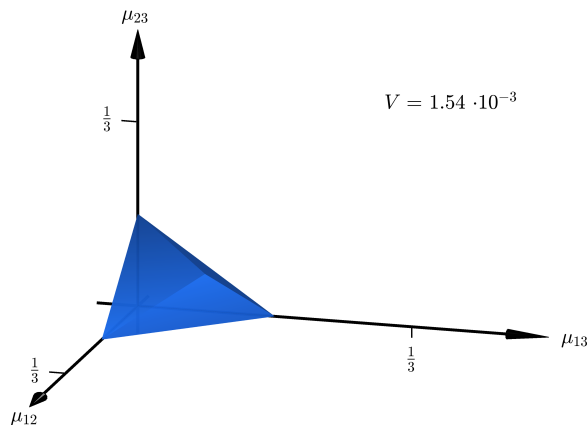


Figure 5: The diamond-shaped polytope $\mathcal{D}_{\infty\text{-rep},\bar{\lambda}}$, as defined in (4.9), is depicted in blue. The elements $(\mu_{ij})_{i,j=1}^3$ of the polytope are parametrized by their off-diagonal entries μ_{12}, μ_{13} and μ_{23} . The volume of $\mathcal{D}_{\infty\text{-rep},\bar{\lambda}}$ is indicated in the upper-right corner.

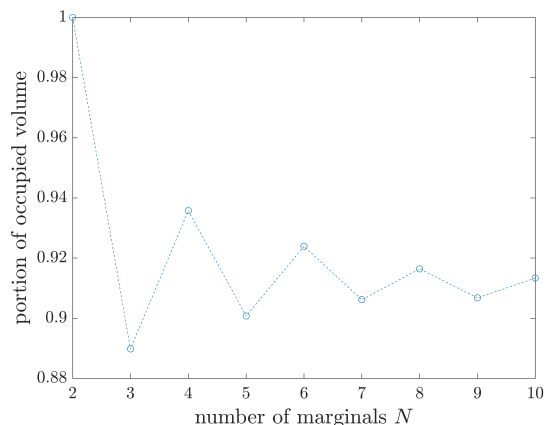


Figure 6: The volumetric ratio, reduced Monge polytope to reduced Kantorovich polytope for N marginals and 3 states, is depicted in dependency of the number of marginals N .

It was proven in [17] that N -representability becomes an increasingly stringent condition as N grows, in more detail, $\mathcal{P}_{N\text{-rep}}(X^2) \subseteq \mathcal{P}_{\hat{N}\text{-rep}}(X^2)$ for any $N \geq \hat{N} \geq 2$. It follows immediately that the reduced Kantorovich polytope for N marginals and 3 states $\mathcal{P}_{N\text{-rep},\bar{\lambda}}(X^2)$ is

contained in the reduced Kantorovich polytope $\mathcal{P}_{\hat{N}\text{-rep},\bar{\lambda}}(X^2)$ for \hat{N} marginals and 3 states. As $\mathcal{P}_{N\text{-rep},\bar{\lambda}}(X^2)$ is closed and convex, $\mathcal{D}_{\infty\text{-rep},\bar{\lambda}}$ is a subset of the reduced Kantorovich polytope $\mathcal{P}_{N\text{-rep},\bar{\lambda}}(X^2)$ for any number $N \geq 2$ of marginals and 3 sites. In summary we get the following chain of inequalities

$$\min_{\mu \in \mathcal{P}_{N\text{-rep},\bar{\lambda}}(X^2)} V[\mu] \leq \min_{\mu \in \mathcal{P}_{(N+1)\text{-rep},\bar{\lambda}}(X^2)} V[\mu] \leq \dots \leq \min_{\mu \in \mathcal{D}_{\infty\text{-rep},\bar{\lambda}}} V[\mu] \leq V[ER^{(\infty)}], \quad (4.10)$$

where $V[\mu] := \int_{X^2} v(x, y) d\mu(x, y)$. The inequalities (4.10) show that for any number of marginals $N \geq 2$ we can find an upper bound of the optimal value in (1.8) by computing the objective value of the 'attractive limit extreme point' $EA^{(\infty)}$, the 'repulsive limit extreme point' $ER^{(\infty)}$ and the 'axis limit extreme points' $E12^{(\infty)}$, $E13^{(\infty)}$ as well as $E23^{(\infty)}$ and choosing the smallest one. Note that this improves the in physics common mean field approximation $V[ER^{(\infty)}]$, where one usually considers repulsive pair-costs $v : X \times X \rightarrow \mathbb{R}$.

Finally, we note that the volume portion of the reduced Kantorovich polytope that is occupied by the reduced Monge polytope exhibits oscillatory behavior with decreasing amplitude when interpreted as a function of the number of marginals N , see Figure 6. The considered volumetric ratio oscillates around a value above 0.9 where even marginals when directly compared to the odd marginals produce a higher ratio. In the sense that an optimizer in the occupied volume yields the existence of a Monge-solution, the Monge ansatz seems to be 'better' for an even number of marginals.

References

- [1] Martial Agueh and Guillaume Carlier. Barycenters in the Wasserstein Space. *SIAM J. Math. Anal.*, 43(2):904–924, 2011.
- [2] Mathias Beiglböck, Pierre Henry-Labordère, and Friedrich Penkner. Model-independent bounds for option prices - a mass transport approach. *Finance Stoch.*, 17(3):477–501, 7 2013.
- [3] Dimitri P. Bertsekas. *Convex Optimization Theory*. Athena Scientific, Belmont, MA, 1 edition, 2009.
- [4] Garrett Birkhoff. Tres observaciones sobre el algebra lineal. *Universidad Nacional de Tucuman Revista, Serie A*, 5(3):147–151, 1946.
- [5] Rainer Burkard, Mauro Dell'Amico, and Silvano Martello. *Assignment Problems. Revised reprint*. Society for Industrial and Applied Mathematics, 2012.
- [6] Giuseppe Buttazzo, Luigi De Pascale, and Paola Gori-Giorgi. Optimal-transport formulation of electronic density-functional theory. *Phys. Rev. A*, 85:062502, 6 2012.
- [7] Guillaume Carlier. On a Class of Multidimensional Optimal Transportation Problems. *J. Convex Anal.*, 10(2):517–529, 02 2003.
- [8] Guillaume Carlier and Ivar Ekeland. Matching for Teams. *Econom. Theory*, 42(2):397–418, 2 2010.

- [9] Guillaume Carlier and Bruno Nazaret. Optimal transportation for the determinant. *ESAIM Control Optim. Calc. Var.*, 14(4):678–698, 2008.
- [10] Huajie Chen, Gero Friesecke, and Christian B. Mendl. Numerical Methods for a Kohn-Sham Density Functional Model Based on Optimal Transport. *Journal of Chemical Theory and Computation*, 10(10):4360–4368, 2014. PMID: 26588133.
- [11] Pierre-André Chiappori, Robert J. McCann, and Lars P. Nesheim. Hedonic price equilibria, stable matching, and optimal transport: equivalence, topology, and uniqueness. *Econom. Theory*, 42(2):317–354, Feb 2010.
- [12] Maria Colombo, Luigi De Pascale, and Simone Di Marino. Multimarginal Optimal Transport Maps for One-dimensional Repulsive Costs. *Canad. J. Math.*, 67:350–368, 2013.
- [13] Codina Cotar, Gero Friesecke, and Claudia Klöppelberg. Density Functional Theory and Optimal Transportation with Coulomb Cost. *Comm. Pure Appl. Math.*, 66(4):548–599, 2013.
- [14] Codina Cotar, Gero Friesecke, and Brendan Pass. Infinite-body optimal transport with Coulomb cost. *Calc. Var. Partial Differential Equations*, 54(1):717–742, 9 2015.
- [15] J. Csima. Multidimensional Stochastic Matrices and Patterns. *J. Algebra*, 14(2):194 – 202, 1970.
- [16] Gero Friesecke. A simple counterexample to the Monge ansatz in multi-marginal optimal transport, convex geometry of the set of Kantorovich plans, and the Frenkel-Kontorova model. *ArXiv e-prints*, 8 2018.
- [17] Gero Friesecke, Christian B. Mendl, Brendan Pass, Codina Cotar, and Claudia Klöppelberg. N-density representability and the optimal transport limit of the Hohenberg-Kohn functional. *The Journal of Chemical Physics*, 139(16):164109, 2013.
- [18] Gero Friesecke and Daniela Vögler. Breaking the Curse of Dimension in Multi-Marginal Kantorovich Optimal Transport on Finite State Spaces. *SIAM J. Math. Anal.*, 50(4):3996–4019, 2018.
- [19] Alfred Galichon, Pierre Henry-Labordère, and Nizar Touzi. A stochastic control approach to no-arbitrage bounds given marginals, with an application to lookback options. *Ann. Appl. Probab.*, 24(1):312–336, 2014.
- [20] Wilfrid Gangbo and Andrzej Świąch. Optimal maps for the multidimensional Monge-Kantorovich problem. *Comm. Pure Appl. Math.*, 51(1):23–45, 1998.
- [21] Augusto Gerolin, Anna Kausamo, and Tapio Rajala. Non-existence of optimal transport maps for the multi-marginal repulsive harmonic cost. *ArXiv e-prints*, 5 2018.
- [22] Henri Heinich. Problème de Monge pour probabilités. *C. R. Math. Acad. Sci. Paris*, 334(9):793–795, 12 2002.
- [23] Lars Hörmander. *Notions of Convexity*. Birkhäuser, Boston, Massachusetts, 1994.

- [24] The MathWorks Inc. *MATLAB and Statistics Toolbox R2018b (MATLAB 9.5)*. Natick, Massachusetts, United States, 2018.
- [25] V. M. Kravtsov. Combinatorial properties of noninteger vertices of a polytope in a three-index axial assignment problem. *Cybernet. Systems Anal.*, 43(1):25–33, Jan 2007.
- [26] Nathan Linial and Zur Luria. On the Vertices of the d-Dimensional Birkhoff Polytope. *Discrete Comput. Geom.*, 51(1):161–170, Jan 2014.
- [27] Abbas Moameni and Brendan Pass. Solutions to multi-marginal optimal transport problems concentrated on several graphs. *ESAIM Control Optim. Calc. Var.*, 23(2):551–567, 2017.
- [28] Brendan Pass. Uniqueness and Monge Solutions in the Multimarginal Optimal Transportation Problem. *SIAM J. Math. Anal.*, 43(6):2758–2775, 2011.
- [29] Brendan Pass. On the local structure of optimal measures in the multi-marginal optimal transportation problem. *Calc. Var. Partial Differential Equations*, 43(3):529–536, Mar 2012.
- [30] Brendan Pass. Remarks on the semi-classical Hohenberg-Kohn functional. *Nonlinearity*, 26(9):2731, 2013.
- [31] The polymake team. *polymake 3.2*. Discrete Mathematics/Geometry Institut für Mathematik der Technischen Universität Berlin, Straße des 17. Juni 136, Berlin, Deutschland, 2018.
- [32] Julien Rabin, Gabriel Peyré, Julie Delon, and Marc Bernot. Wasserstein Barycenter and Its Application to Texture Mixing. *Scale Space and Variational Methods in Computer Vision*, pages 435–446, 2012.
- [33] R. Tyrrell Rockafellar. *Convex Analysis*. Princeton University Press, New Jersey, 1997.
- [34] Frits C. R. Spijksma. *Multi Index Assignment Problems: Complexity, Approximation, Applications*, pages 1–12. Springer US, Boston, MA, 2000.
- [35] Cédric Villani. *Optimal Transport: Old and New*. Springer Verlag, Berlin Heidelberg, 2009.
- [36] John von Neumann. A certain zero-sum two person game equivalent to the optimal assignment problem. *Contributions to the Theory of Games*, 11:5–12, 1953.